

# Factorisation of laser pulse ionisation probabilities in the multiphotonic regime

**R. Della Picca, J. Fiol and P. D. Fainstein**

CONICET and Centro Atómico Bariloche, Comisión Nacional de Energía Atómica,  
Avda E. Bustillo 9500, 8400 Bariloche, Argentina

E-mail: renata@cab.cnea.gov.ar

**Abstract.** We present a detailed study of the ionisation probability of H and  $\text{H}_2^+$  induced by an short intense laser pulse. Starting from a Coulomb-Volkov description of the process we derive a multipole-like expansion where the first order transition matrix may be factored into two contributions: one that accounts for the effect of the electromagnetic field on the free-electron final-state and a second factor that depends only on the target structure. Such a separation may be valuable to solve complex atomic or molecular systems as well as to interpret the dynamics of the process in simpler terms. We show that the series expansion converges rapidly, and thus the inclusion of the first few terms are sufficient to produce accurate results.

## 1. Introduction

The interaction of strong and short laser pulses with atoms and molecules has received renewed attention in the recent past, both experimentally and theoretically [1–5], mainly because the advances in laser technology have made feasible time-resolved measurements of atomic and molecular processes. These advances made possible new experimental investigations of atomic and molecular processes on an ultrashort time-scale, and under ultra intense laser radiation. These techniques lead the way to measurement of highly nonlinear phenomena, and even their control is now possible [6–8].

On the theoretical side, since the first works by Kulander [9, 10], more than two decades ago, many computational techniques have been developed to solve the three-dimensional time-dependent Schrödinger equation (TDSE) for single-electron systems [11–14]. The advances in computing power allows us to perform these computations in a question of minutes nowadays. However, the computation power demands imposed by precision numerical solutions of the Schrödinger equation quickly scales out-of-reach when the complexity of the systems increases.

Alternative, complementary approaches based on perturbative expansions could provide results at relatively low-computer cost at the expense of some precision-loss. Traditionally, the Keldysh-Faisal-Reiss or Strong-Field Approximation (SFA) [15–17] (see also [3]) has been employed to theoretically describe these processes when the field is intense. On the contrary, when the field is weak, a First Order Perturbation theory (FPA) is sufficient to describe the process [18]. In the intermediate regime, where the interaction of the electrons with the nucleus and with the electromagnetic (EM) field are of similar strength, none of the potentials may be neglected. To describe ionisation processes in this regime was developed the Coulomb-Volkov approximation (frequently called CV2 or CVA) [19–22], where both interactions with the ejected electron are taken into account at the same level in the final-state.

The CVA approach has been widely used to investigate the ionisation of atomic hydrogen [22–24], alkali metal atoms [25], simple molecules [26] and positronium [27]. Furthermore, there are several implementations of the Coulomb Volkov approximation, that may be used in a wide range of conditions: the renormalised CV (RCV) extends the CVA to the non-perturbative regime [28], the modified CV (MCV) introduces the coupling to intermediate bound states [29], and the doubly distorted CV (DDCV) [30, 31] includes the distortion by the laser field also in the initial state.

Alternatively, Dimitrovski *et. al.* [32, 33] have presented analytical formulas for ionisation by very short pulses, that are independent of the laser intensity, in the context of First Magnus Approximation (FMA). When weak and short field are applied, FPA and FMA can be used to obtain the sudden approximation [18, 32] where the ionisation amplitude is proportional to the momentum transfer and the dipole transition matrix.

The interaction with intense laser fields could induce, besides multiphoton ionisation (MPI), another important phenomenon: High order Harmonic Generation (HHG). In a semiclassical recollision picture it proceeds in three steps: first the electron

is released from the target, then the electron interacts with the laser field, and in a third step, if the electron returns to the atom, radiative recombination may take place. Alternatively, in the third step, an elastic scattering or an (e,2e) process may take place, giving place to High-order Above-Threshold Ionisation (HATI) or Non-Sequential Double Ionisation (NSDI), respectively [5, 34].

Despite the well-known shortcomings of the Strong Field Approximation (SFA), such as the discrepancies for calculations on different gauges, three-steps processes may be understood within its simple framework. The first-order SFA is able to describe ‘direct’ ionisation, but a second order term is necessary to include the post-ionisation interaction between the free electron and the target. In contrast, this mechanism is already included in the first-order CVA, providing both direct and rescattering amplitudes [3]. Recently, an alternative approach to this problem, called Quantitative Rescattering theory (QRS), was developed by Lin *et. al.* [34]. In this approach the yields for HHG, HATI and NSDI can be expressed as the product of the returning electron wave packet probability with photo-recombination, elastic electron scattering, and electron-impact ionisation cross sections, respectively. Also recently, in a full quantum mechanical description, Frolov *et. al.* have deduced an analytical factorisation of the spectra in terms of an electron wavepacket and the cross-section of photo-recombination (for HHG), and elastic electron scattering (for HATI), see [35–37] and references therein.

This type of yield factorisation allows the study of more complex atoms or molecules, by separating the roles of the laser-pulse and the parent-ion, and allowing to accurately extract information about the target, (see for example [34, 38–40]) offering a promising tool for dynamic chemical imaging with temporal resolution of few femtoseconds.

In this work we study the above threshold ionisation (ATI) of atomic hydrogen by short laser pulses within the CVA approach. We derive an expansion of the transition matrix in powers of the laser-field vector potential, whose first term is sufficient to describe ionisation in the multiphotonic regime. This first-order term is written as the product of an one-photon ionisation transition-matrix and an integral factor depending on the laser pulse.

We compare the ATI spectra with TDSE results and analyse the convergence of the expansion, how each factor of this approximation contributes to the electronic spectra, and present some useful applications of this factorisation. Finally, we also investigate the ionisation from some excited states of the hydrogen atom, and from  $H_2^+$  employing exact wavefunctions for both the initial and final channels.

Atomic units are employed, except where otherwise stated.

## 2. Review of the Coulomb-Volkov approximation

Let us consider the ionisation of an atomic or molecular system by interaction with a finite laser pulse of duration  $\tau$ . In the length gauge, the action of the pulse may be described as a time-dependent force produced by the electric field. Thus, the time-

dependent Schrödinger equation (TDSE) reads

$$i \frac{\partial \Psi(\mathbf{r}, t)}{\partial t} = \left[ \frac{\hat{\mathbf{p}}^2}{2} + V(\mathbf{r}, t) + \mathbf{F}(t) \cdot \mathbf{r} \right] \Psi(\mathbf{r}, t). \quad (1)$$

We consider a finite laser pulse, that exerts a force on the system given by its electric field

$$\mathbf{F}(t) = F_0 \sin(\omega(t - t_0)) \sin^2(\pi t / \tau) \hat{\epsilon} \quad (2)$$

for  $0 < t < \tau$ , and that vanishes at all other times. The pulse is characterized by its central frequency  $\omega$ , the pulse duration  $\tau$ , the polarisation vector  $\hat{\epsilon}$ , and the phase-shift, chosen as  $\omega t_0 = (\omega\tau - \pi)/2$  for symmetric pulses.

While the perturbation vanishes outside the time-interval  $\Delta T = (0, \tau)$  we can write the ionisation transition-matrix, in its prior form, as

$$T_{fi}^- = -i \int_0^\tau \langle \Psi_f^-(t) | \mathbf{F}(t) \cdot \mathbf{r} | \phi_i(t) \rangle dt. \quad (3)$$

Here  $\Psi_f^-(t)$  is the exact wavefunction for the final state with ingoing boundary conditions, and  $\phi_i(t)$  is the asymptotic target wavefunction in absence of external fields.

The double differential ionisation probability in energy and angle of the emitted electron is obtained from the transition matrix magnitude as

$$\frac{dP_{fi}}{dE d\Omega} = k |T_{fi}|^2. \quad (4)$$

The Coulomb-Volkov approximation (CVA) is obtained by replacing the exact final wavefunction  $|\Psi_f^-(\mathbf{r}, t)\rangle$  by a product of factors corresponding to the solution of two separated problems: one for the isolated field-free atom and one containing the effects of the electron evolving in the external electromagnetic (EM) field. In order to get the correct asymptotic behaviour the plane-wave part must be corrected [19, 20]. This procedure is similar to the one carried-out in continuum-distorted-wave (CDW) theories developed for ion-atom collisions many years ago [41–43]. In this approximation the final-state wavefunction takes the form [19, 20]

$$\chi_f^-(\mathbf{r}, \mathbf{k}, t) = \frac{e^{i\mathbf{k} \cdot \mathbf{r}}}{(2\pi)^{3/2}} D_C^-(\mathbf{k}, \mathbf{r}) D_{\mathbf{A}}^-(\mathbf{k}, \mathbf{r}, t) e^{-iE_f t} \quad (5a)$$

$$D_C^-(\mathbf{k}, \mathbf{r}) = (2\pi)^{3/2} e^{-i\mathbf{k} \cdot \mathbf{r}} \varphi_f^-(\mathbf{r}) \quad (5b)$$

$$D_{\mathbf{A}(t)}^-(\mathbf{k}, \mathbf{r}, t) = e^{i\mathbf{A}(t) \cdot \mathbf{r}} \exp \left[ \frac{-i}{m} \mathbf{k} \cdot \int_\tau^t \mathbf{A}(t') dt' \right] \\ \times \exp \left[ -i \frac{1}{2} \int_\tau^t (A(t'))^2 dt' \right] \quad (5c)$$

$$\mathbf{A}(t) = - \int_\tau^t \mathbf{F}(t') dt' \quad (5d)$$

Here  $\varphi_f^-(\mathbf{r})$  is the final-state of the electron ejected with momentum  $\mathbf{k}$ , corresponding to energy  $E_f = k^2/2$ , and with ingoing wave boundary conditions. We have explicitly set

$m = 1$  and  $Z = -1$  for the electron mass and charge, respectively. For a pure Coulomb potential interaction (hydrogen atom) the distortion factor takes the familiar form:

$$D_C^-(\mathbf{k}, \mathbf{r}) = N^-(\nu) {}_1F_1(i\nu; 1; -i(kr + \mathbf{k} \cdot \mathbf{r})) ,$$

where the normalization factor is defined is given by  $N^-(\nu) = \Gamma(1 - i\nu)e^{-\pi\nu/2}$ , and  $\nu = -1/k$  is the Sommerfeld parameter. For general, more complex, targets the distortion factor must be obtained numerically, and is defined in terms of the final-state target eigenfunction  $\varphi_f$  as given by (5b).

After some manipulation, the CVA transition matrix may be written as [21, 22]

$$T_{fi}^{CV} = f(0)g(0) + \int_0^\tau dt h(t) f(t) g(t) \quad (6a)$$

where

$$h(t) = i (\omega_{fi} + \mathbf{k} \cdot \mathbf{A}(t) + \mathbf{A}^2(t)/2) , \quad (6b)$$

$$f(t) = \exp \left( \int_\tau^t h(t') dt' \right) , \quad (6c)$$

$$g(t) = \int d\mathbf{r} \varphi_f^*(\mathbf{r}) \exp(-i\mathbf{A}(t) \cdot \mathbf{r}) \varphi_i(\mathbf{r}) , \quad (6d)$$

and  $\omega_{fi} = E_f - E_i$ . For symmetric pulses  $A(\tau) = 0$ , and an additional term involving  $g(\tau)$  in the above expression, vanishes due to the orthogonality of the initial and final wavefunctions.

This approximation has been successfully employed to describe atomic ionisation by short UV laser pulses. However its validity is limited to the perturbative regime, where the probability of ionisation is small. It has been shown that the approximation fails when the photon energy is smaller than the ionisation potential  $\omega \ll I_p$ . In order to extend the range of applicability of the theory it has been developed a modified version that includes intermediate bound states [24, 29].

### 3. Multipolar expansion of the T-matrix

It has been shown that the probability may be evaluated efficiently, rendering good results with relatively low computational cost in the case of atomic hydrogen. However, its extension to more complex systems such as many-electron atoms or even small molecular ions can considerably increase computation times. It is desirable to develop approximations that keep the good performance of the CVA but may be applied to laser-induced ionisation of large molecules.

In the range of applicability of the CVA theory, the amplitude of the field  $F_0$  is small and  $\omega > I_P$ . Then, in most cases the magnitude of the vector field  $\mathbf{A}(t)$  is also small. In that case we may expand the exponential in  $g(t)$  in (6d) and keep only the first, most significant, terms

$$\exp(-i\mathbf{A} \cdot \mathbf{r}) = 1 - i\mathbf{A} \cdot \mathbf{r} - \frac{1}{2}(\mathbf{A} \cdot \mathbf{r})^2 + \dots$$

We obtain a series expansion for the transition matrix  $T_{fi}^{CV} = T^{(0)} + T^{(1)} + T^{(2)} + \dots$ , whose first terms are given by

$$T^{(0)} = \langle \varphi_f^- | \varphi_i \rangle \quad (7a)$$

$$T^{(1)} = -i \mathbf{L}^{(1)} \cdot \left[ f(0) \mathbf{A}(0) + \int_0^\tau dt f(t) h(t) \mathbf{A}(t) \right] \quad (7b)$$

$$T^{(2)} = -\frac{1}{2} L^{(2)} \left[ f(0) A^2(0) + \int_0^\tau dt f(t) h(t) A^2(t) \right] \quad (7c)$$

where we have defined the matrix elements  $\mathbf{L}^{(1)} = \langle \varphi_f^- | \mathbf{r} | \varphi_i \rangle$  and  $L^{(2)} = \langle \varphi_f^- | (\hat{\mathbf{e}} \cdot \mathbf{r})^2 | \varphi_i \rangle$ .

Keeping only the first non-vanishing order allows us to decouple the results as two factors from very different origin, one of them accounts for the laser perturbation and its effect on the final state while the other is sensitive to the target structure:

$$T^{(1)} = -i \mathbf{L}^{(1)} \cdot \mathbf{M}^{(1)}, \quad (8)$$

where  $\mathbf{L}^{(1)}$  is the one-photon ionisation transition matrix, and

$$\mathbf{M}^{(1)} = \int_0^\tau \mathbf{F}(t) f(t) dt. \quad (9)$$

The above approximation relies on the condition  $\mathbf{A}(t) \cdot \mathbf{r} \ll 1$ , for that reason we call it *dipole approximation* or DipA. While the amplitude of the vector potential  $\mathbf{A}(t)$  is proportional to the electric field amplitude  $F_0$  and inversely proportional to the frequency  $\omega$ , the range of validity of the approximation is constrained by these two parameters. In principle some of these constraints are already considered in Coulomb-Volkov approximations. It has been shown that the CV2 approximation provides reliable results of atomic and molecular ionisation by ultraviolet lasers whenever the laser intensity is compatible with the perturbation regime and the photon energy is higher than the electron binding energy [22, 29]. However, for a given EM field this approximation may fail as highly-excited states are considered, because the radius of the atomic or molecular system increases. We note that this approximation may also be obtained by neglecting the first factor in the Volkov state (5c). Because this factor contains the spatial dependency of the EM field, space and time are then decoupled in the transition matrix integrals (3).

The Keldysh parameter  $\Gamma \equiv \sqrt{I_p/2U_p} \sim 1$  defines the limit between multiphotonic and tunneling regimes for ionisation processes. Here the ionisation potential energy is  $I_p$  and the ponderomotive energy  $U_p = F_0^2/4\omega^2$ . Then we expect that DipA will work well in the multiphotonic regime, when  $\Gamma \gg 1$ , since in this case  $A \sim 1/\Gamma$  will be small.

To analyse the spectra obtained in DipA we study the different factors in (8). As we mentioned before,  $\mathbf{L}^{(1)}$  is the ionisation transition matrix due to the absorption of one fictitious photon with frequency  $\omega_{fi} = E_f - E_i$ . For eigenfunctions of the unperturbed Hamiltonian, the matrix element can be written equivalently either in the length or velocity gauge:

$$\mathbf{L}^{(1)} = \langle \varphi_f^- | \mathbf{r} | \varphi_i \rangle = -\frac{1}{\omega_{fi}} \langle \varphi_f^- | \nabla | \varphi_i \rangle \quad (10)$$

This term does not contain any information on the EM field, and will be the same for all laser pulses. On the other hand, since the function  $f$  can be factorised as  $f(t) = j(t) \exp(i\omega_{fi}t)$ , the contribution of the field can be written as

$$\mathbf{M}^{(1)} = \int_0^\tau dt \mathbf{F}(t) j(t) e^{i\omega_{fi}t} \quad (11)$$

Here  $j(t)$  is the part of the Volkov state that is taken into account in DipA and a phase that could be omitted:

$$j(t) = e^{-i\omega_{fi}\tau} \exp \left[ i \mathbf{k} \cdot \int_\tau^t \mathbf{A}(t') dt' \right] \times \exp \left[ \frac{i}{2} \int_\tau^t (A(t'))^2 dt' \right] \quad (12)$$

Equation (11) have the aspect of a Fourier transform. However, the function  $j$  and the *Fourier frequency*  $\omega_{fi}$  are not independent, since both depends on the electron energy  $E_f$ . For sufficiently low intensity of the field,  $j \sim 1$  and this equation defines exactly the Fourier transform of the EM pulse. Also, we note that the only information about the target that  $\mathbf{M}^{(1)}$  contains is the energy  $E_i$  in  $\omega_{fi}$ . For this reason, spectra for different targets, or initial states with different binding energies can be reproduced approximately, by shifting the final electron energy.

In the following sections we analyse the present multipolar expansion. We present the CVA spectra for H atoms and  $\text{H}_2^+$  molecular ions, comparing with TDSE results and the spectra obtained employing the first- and second-order transition matrix in the multipolar expansion of CVA.

## 4. Spectra for H

### 4.1. Comparison of different theories

In this section we compare CVA and DipA spectra to the results obtained solving the TDSE with the code QPROP [12]. For CVA calculations we employed equations (4) and (6a), while in the DipA case we considered (4) and (8).

In figures 1, 2 and 3 we present the density of probability (DOS) for the ionisation of atomic hydrogen (1s). The spectra, as function of the electron energy, were obtained integrating over all electron-emission directions. We consider laser pulses of intensity  $F_0 = 0.05$  a.u., duration corresponding to  $N = 1, 7$  and 27 cycles, and frequencies  $\omega = 0.855$  (Fig. 1), 1.71 (Fig. 2), and 0.427 a.u. (Fig. 3). The results for  $N = 1$  and 27 are multiplied by 10 and  $10^{-2}$ , respectively, for better visualisation.

In general, we observe from these figures a good agreement between CVA, TDSE and DipA results, specially for high laser frequencies. These examples are within the limits of applicability of the CVA approximation; thus they are almost indistinguishable from the numerically exact results given labelled TDSE. At lower frequencies the disagreement between CVA and TDSE has been analysed by Duchateau *et. al.* [21, 22], and they pointed out that the CVA fails because it does not consider transitions to

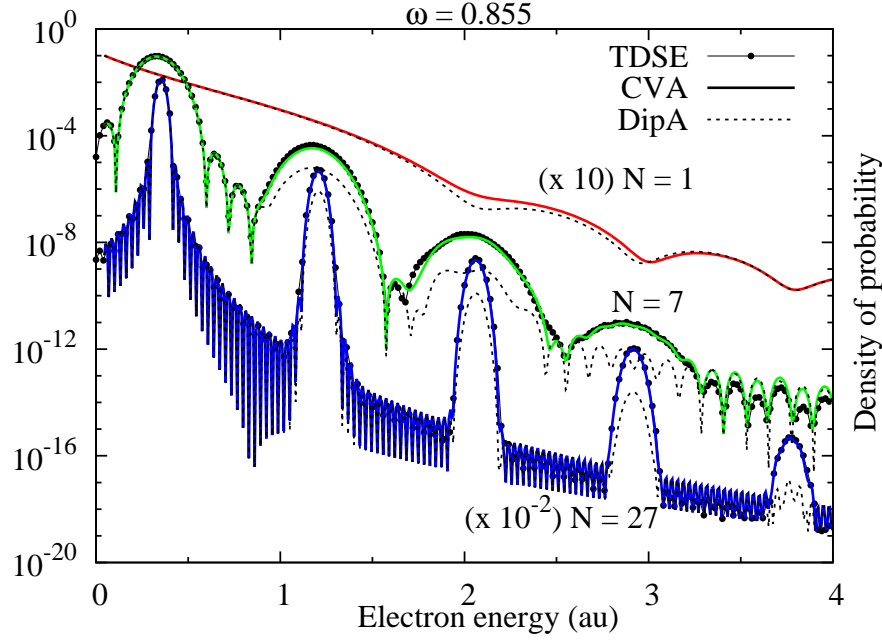


**Figure 1.** (colour online) Electron spectra for ionisation of H(1s) as function of the ejected electron energy for a laser pulse with  $N = 1$  (up),  $N = 7$  (middle) and  $N = 27$  (bottom) cycles. Laser frequency  $\omega = 0.855$  a.u.,  $F_0 = 0.05$  a.u. ( $\Gamma = 17.1$ ). Full line: CVA, dotted line: Dipole Approximation (DipA) and full line with circles: TDSE results.

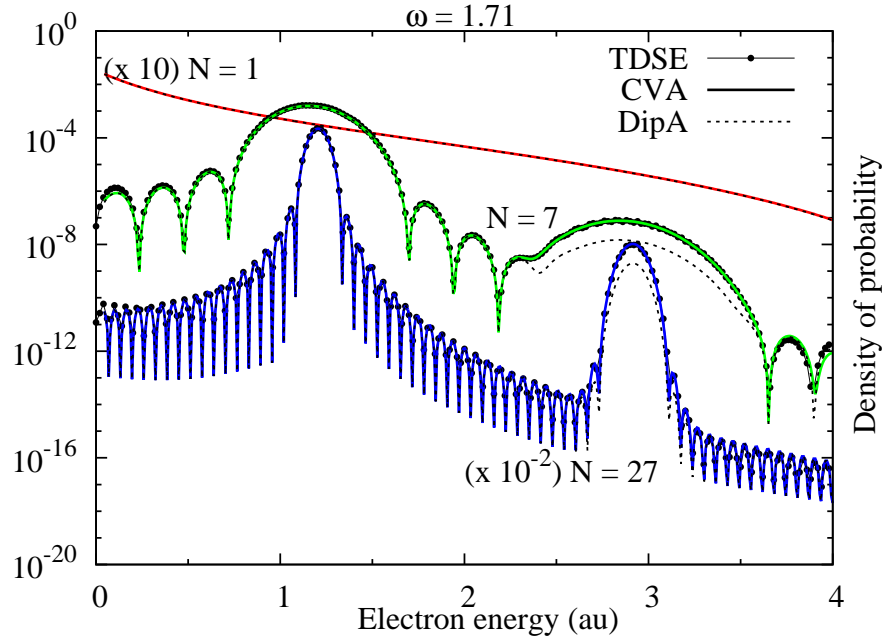


**Figure 2.** (colour online) Idem Fig. 1 with  $\omega = 1.71$  a.u. ( $\Gamma = 34.2$ )

intermediate excited states. This mechanism is more important when the ionisation energy is larger than the laser frequency.

Also, we observe the formation of above-threshold-ionisation (ATI) peaks when

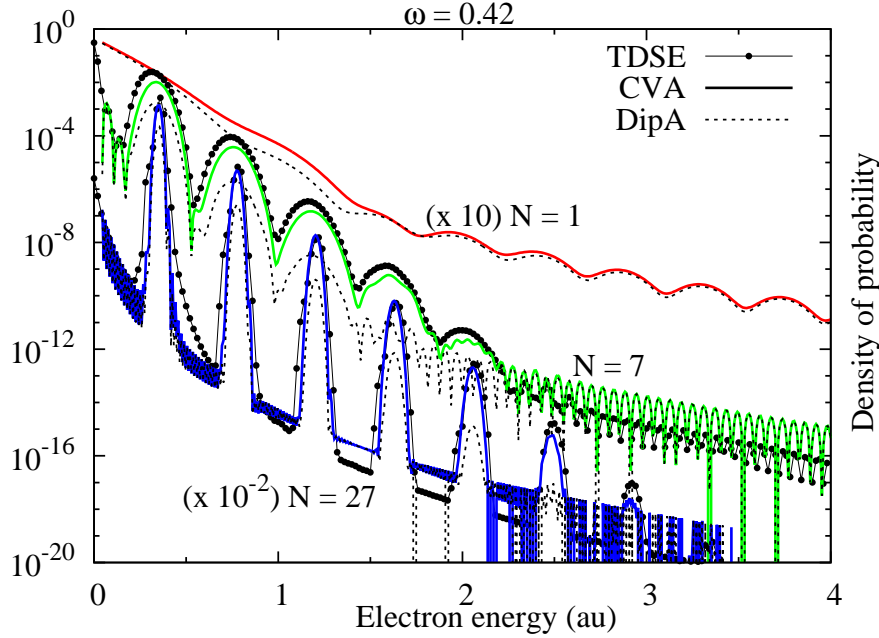


**Figure 3.** (colour online) Idem Fig. 1 with  $\omega = 0.427$  a.u. ( $\Gamma = 8.55$ )

increasing the number of cycles of the pulse. These structures correspond to the absorption of  $n$  photons at the value energy  $E_n = E_i + n\omega - U_p$  (see for example [3]).

#### 4.2. Analysis of DipA

Let us now discuss the DipA results, plotted with dotted line in figures 1 to 3. In these figures we observe that the shape of the spectra is well reproduced by the dipole approximation, but there are disagreements in the ATI peaks, corresponding to multiple-photon absorption, where DipA underestimates the ionisation probabilities. In all cases, the first peak, that is the most important in magnitude, is well reproduced by the DipA. As a consequence, total ionisation probabilities are accurately given by this approximation. This is observed in figure 4, where we show total ionisation probabilities for a frequency  $\omega = 0.855$  a.u., as function of the laser pulse duration, and for several EM intensities. We can observe that the first-order approximation (DipA) reproduces very well the full calculations in a very extended range of laser pulse parameters.

As we mentioned before, the intensities of the secondary ATI peaks are not well described by DipA. This means that in this regions there are couplings between time and space, and/or the exponential factor  $\exp(-i\mathbf{A} \cdot \mathbf{r})$  plays a crucial role in the description of the ionisation spectra.

The  $\omega = 0.427$  a.u. case of figure 3 is a bit different since the ATI peaks are closer to each other and shifted to the left. The first peak would appear at negative energies, below the ionisation threshold. Thus, the first peak corresponds to the absorption of two photons, showing worse agreement. This is an expected result, according with the

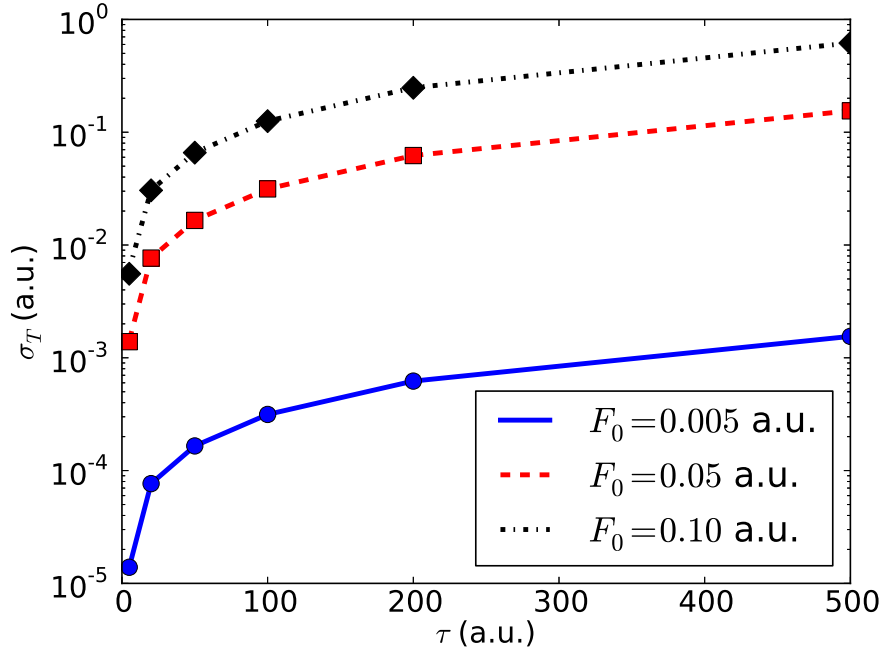


**Figure 4.** Comparison of hydrogen (1s) total ionisation probabilities by pulses laser of frequency  $\omega = 0.855$  a.u., for several different intensities. Lines correspond to full CVA calculations, while symbols were obtained in the first order DipA.

above description, for low frequencies or high amplitudes  $A$ .

We note that for large electron energies, outside the ATI peaks, the background of the spectra is also well reproduced. This fact can be explained noting that for high energies the contribution of the term  $\mathbf{k} \cdot \int \mathbf{A}(t) dt$  is more important than the contribution of  $\mathbf{r} \cdot \mathbf{A}$ . Then, this last term can be omitted in the exponential of the Volkov state (5c), resulting precisely in DipA.

Surprisingly, short pulses corresponding to  $N = 1$  cycle are well reproduced by DipA independently of the laser frequency (figures 1 to 3). For very short pulses and in the context of the First Magnus Approximation (FMA), Dimitrovski *et al.* [32, 33] found that the ionisation amplitude is independent of the pulse shape and, therefore, all pulses are equivalent if they have the same value of  $\mathbf{A}(0)$ . In connection with the present Dipole Approximation, we note that pulse amplitudes  $\mathbf{A}(t)$  that vary slowly in time allow naturally the decoupling of spatial and temporal integrals in the transition matrix.

Furthermore, when for short pulses and weak fields, FMA and first order perturbation theory (FPA) can be combined to give rise to the *sudden approximation* [18, 32], where the ionisation amplitude is described by (8), but simplifying  $f(t) = 1$  in (9). Our proposed DipA presents the same type of benefits that the sudden approximation, but for a extended range of laser parameters, as we can observe in figure 4.

### 4.3. DipA applications

DipA enable us to understand the features of the spectra, allowing us to separate those that come from the pulse from those that are exclusively due to the nature of the target. For example, because we consider ionisation of H atoms from the ground state in the cases presented in figures 1 to 4, in all cases the contribution of  $\mathbf{L}^{(1)}$  is the same. Its squared modulus, integrated in electron emission direction, is proportional to the photoionisation cross-section and is a monotonically decreasing function of the energy (see for example eq. 37 of [44]).

On the contrary, the factor  $\mathbf{M}^{(1)}$ , is different for each of the nine spectra plotted in figure 1 to 3, corresponding to the nine different laser pulses. For symmetric pulses with  $N = 1$  cycle, the shape of the pulse is basically a peak, then the Fourier transform predicts a widely spread spectra, as observed from the above figures. Increasing the number of cycles, the Fourier transform of the pulse narrows considerably, as a delta-like function, evaluated in the central frequency of the pulse. This behavior gives rise to the first ATI peak. To analyse the formation of the others ATI peaks we can expand the exponential in  $j(t)$  in powers of the argument. Each of these terms contributes to an harmonic of the original pulse, for this reason his Fourier transform shows the ATI peaks centered in positions that are multiples of the central frequency  $\omega$ . Also, when increasing the intensity of the pulse, more terms in the exponential expansion are needed, explaining the formation of new ATI peaks as the intensity increases (see for example figure 1 of [22]).

Summarising, we can note that the general shape of the spectra is defined by  $\mathbf{M}^{(1)}$ : the number of ATI peaks, their amplitude and width could be estimated from the analysis of this factor, as well as the dependence on the carrier envelope phase (CEP), fixed to  $\omega t_0$  in this work.

One important application of this approximations is its use in more complex systems, like molecules. In this case it is possible to construct the spectra for laser pulse ionisation by multiplying the one-photon ionisation transition-matrix of this complex system by the factor  $\mathbf{M}^{(1)}$  with the information of the pulse. For sufficiently high-frequency pulses, as the generated from typical HHG spectra [45–48], this approximation will be valid. Conversely, knowing the emission spectra of an unknown target interacting with such pulses it is possible to decompose the spectra, as proposed in DipA, and obtain information about the target. This type of experiment where the extreme-ultraviolet attosecond light-pulse are used as source to emit electrons and obtain “tomographic images” of the target have been achieved recently [8, 49, 50].

Another interesting application of the DipA is its application to a simpler Strong Field Approximation (SFA). The first order of SFA in length gauge (LG SFA) can be obtained replacing the coulomb wave function  $\varphi_f^-$  by a plane-wave in the present CVA calculations. It is known that this approximation may overestimate the exact results and needs to be renormalised [21]. However, it is possible to employ SFA with the DipA factorisation in the regime where DipA works well ( $\Gamma \gg 1$  and  $\omega > I_p$ ). Since

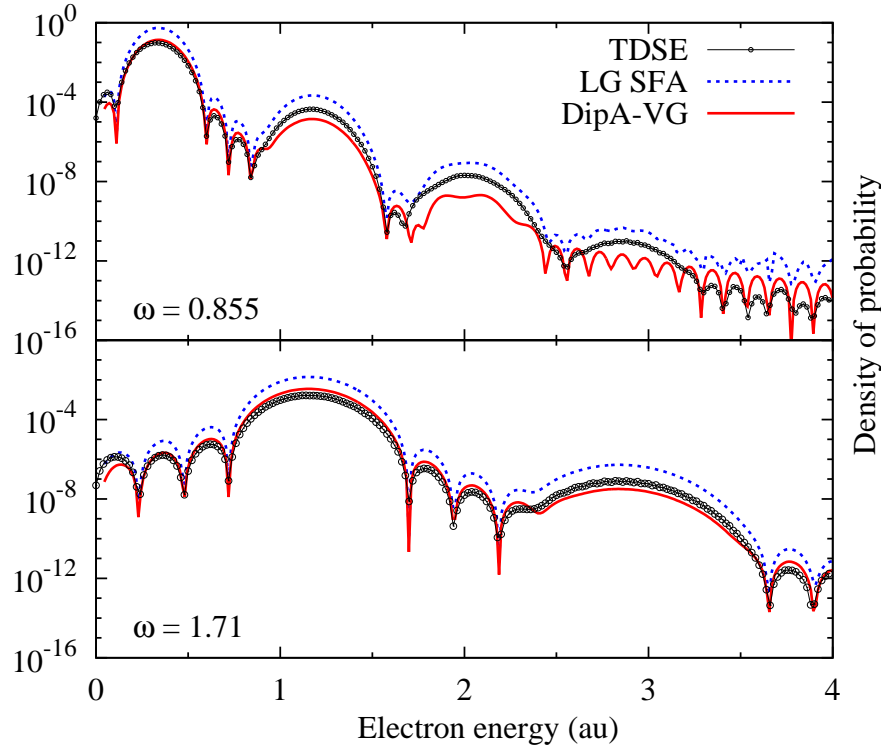


**Figure 5.** (colour online) Ionisation spectra for  $H(1s)$  for laser pulses with  $\omega = 0.855$  (up) and  $1.71$  a.u. (down),  $N = 7$  cycles and  $F_0 = 0.05$  a.u. Full line (red): DipA-GV (SFA) see text. Dotted line (blue): first order LG SFA. Full line with circles (black): TDSE results.

the plane-wave is not an eigenfunction of the unperturbed Hamiltonian the result will depend on the choice of gauge in the one-photon ionisation transition-matrix (10). The length gauge in  $\mathbf{L}^{(1)}$  gives similar results that LG SFA. On the other side, when  $\mathbf{L}^{(1)}$  is calculated in the velocity gauge, the resulting spectra magnitudes are reduced to values similar to those obtained by solving numerically the TDSE.

In figure 5 we compare the TDSE results with those for LG SFA, and with DipA-VG (SFA) results (8). For the DipA factorization, we employed plane-waves in the final-state and velocity gauge i.e. the right-side of (10).

We observe that LG SFA spectra are at least one order of magnitude higher than the exact results while the velocity gauge in DipA-VG reduces considerably this difference, specially at the first peak where there is the major contribution to total ionisation probabilities. For the highest frequency investigated, DipA-VG gives almost the same spectra that TDSE while LG SFA remains one order of magnitude larger.

There has been long standing discussions about the accuracy of different gauges in SFA [51, 52], that have recovered interest in recent years (see for example [53–56] to cite just a few), and deserves to be treated in a separated work. Nevertheless, here we simply note that in the multiphotonic regime, in the region of applicability of DipA, SFA calculations could be improved by choosing the velocity gauge in the computation of the factor  $\mathbf{L}^{(1)}$ .

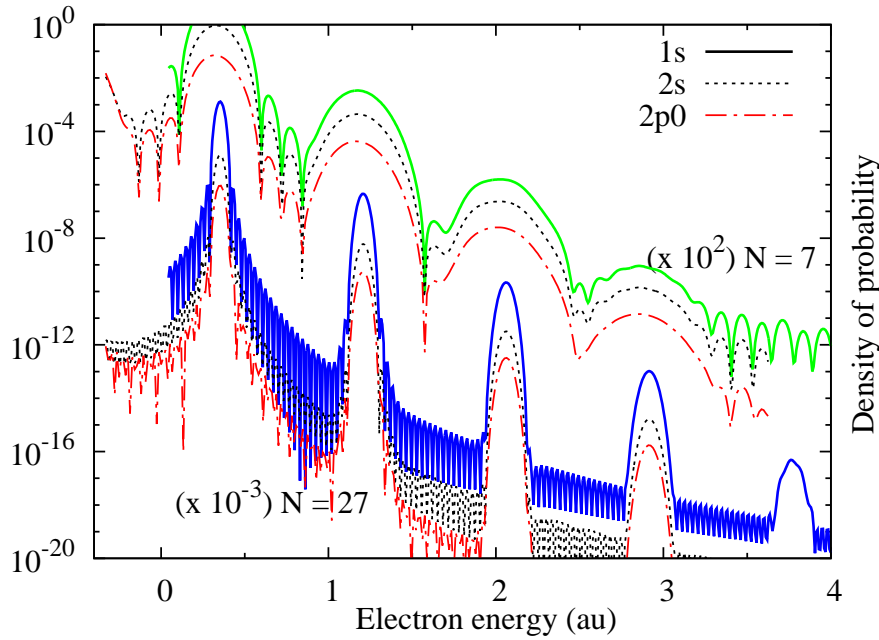


**Figure 6.** (colour online) Ionisation spectra for H from 1s solid line, 2s dotted line and  $2p_0$  dashed dotted line for laser pulses with  $\omega = 0.855$  a.u.,  $F_0 = 0.05$  a.u.,  $N = 7$  and 27 cycles. The ionisation spectra from 2s and  $2p_0$  are shifted to lower energy in 0.375 a.u.

#### 4.4. Ionisation from excited states and 2<sup>nd</sup>-order approximation

In this section we want to analyse the spectra for ionisation of hydrogen atoms from excited states. In figure 6 we present CVA ionisation probabilities for H atoms from the 1s, 2s and  $2p_0$  states. For the excited state we shifted the spectra in energy  $E_1 - E_2 = -0.375$  a.u. As a result, the energy position of the ATI peaks for the different spectra are matched. We observe that the shape of the spectra are very similar in all cases, but the ionisation probabilities are lower for excited states. These facts can be understood in the DipA context: as we discussed before, the effect of the target on  $\mathbf{M}^{(1)}$  produces a shift in the spectra that we have just corrected. Additionally, the intensity of the spectra is modulated by the different one-photon transition-matrices  $\mathbf{L}^{(1)}$  in each case.

Also, in figure 7 we show the ionisation probabilities from H(2s), comparing the CVA results with DipA. Like in the 1s case (see figure 1), DipA underestimates the magnitude of ATI peaks for multiple photon absorption. Evidently, the first non-vanishing term in the multipolar expansion of the T-matrix is not enough to describe the ionisation process. In order to achieve a better representation we include a second term, i.e.  $T \approx T^{(1)} + T^{(2)}$  (see (7a)) in the differential ionisation probability (4). This calculation is also presented in figure 7, labelled as second-order (2<sup>nd</sup> T). We observe that the addition of the second term is sufficient to reproduce accurately the spectrum in an extended energy range. Visible differences appear only at high electron energies, at the third ATI peak.

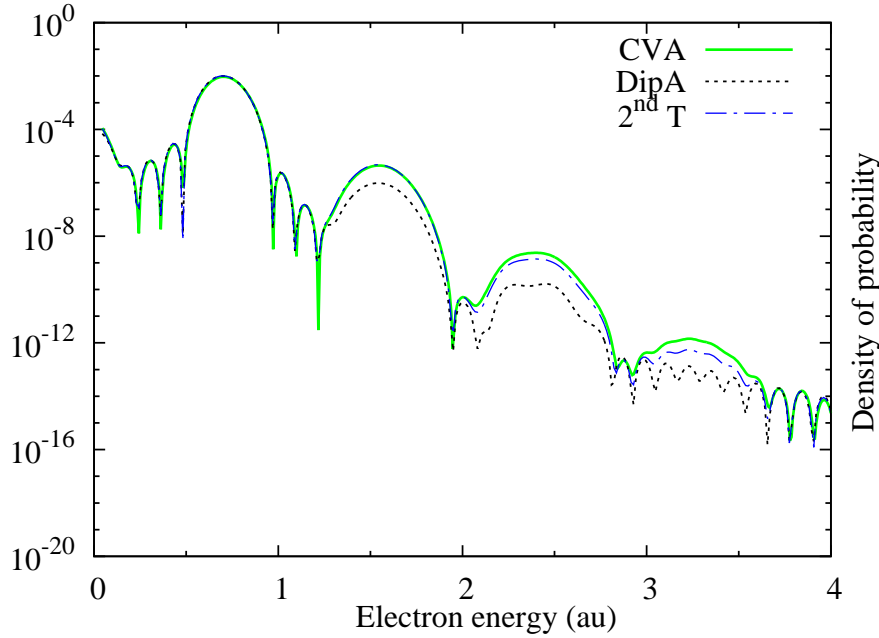


**Figure 7.** (colour online) Ionisation spectra for H from 2s for laser pulses with  $\omega = 0.855$  a.u.,  $F_0 = 0.05$  a.u. and  $N = 7$  cycles. Full line (green): CVA, dotted line (black): DipA and dashed dotted line (blue): 2<sup>nd</sup> order calculations.

## 5. Spectra for $\text{H}_2^+$

In this section we study the ionisation of fixed-in-space  $\text{H}_2^+$  molecular ions by short laser-pulses. The nuclei of the molecule, having charges  $Z_a = Z_b = 1$ , are fixed at the internuclear distance  $R = 2$  a.u. Employing spheroidal coordinates and using standard computational methods we calculate exactly the initial bound  $\varphi_i(\mathbf{r})$  [57], and final continuum  $\varphi_f^-(\mathbf{r})$  [58, 59] states of the molecule. Also the plane-wave  $\exp(-i\mathbf{A}(t) \cdot \mathbf{r})$  is expressed in spheroidal coordinates [44, 60]. With these wave functions the factor  $g(t)$  in (6d) is evaluated numerically for the CVA calculation. To obtain DipA spectra,  $\mathbf{L}^{(1)}$  is computed in the same way that in previous works [44, 61, 62].

In figure 8 we present the ionisation probability differential in energy and angle, for forward configuration, i.e: the emission direction is parallel to the internuclear axis and both are parallel to the polarisation vector (see figure 9(a)). As before, there is good agreement between the CVA and DipA calculations for all the energy-range investigated.

Overall, the spectra for molecular ionisation are similar to the ones presented for atoms (figure 1 and 2), but there are some notable differences:

- (1) The spectra are energy-shifted due to different ionisation potentials of the targets. The computed  $1s\sigma$  electronic energy is  $-1.1$  a.u.  $+ 1/R = -16.3$  eV. Since we are considering fixed nuclei, the term  $1/R$  is also present in the energy of the final continuum state. Then, the net shift in the spectra respect the atomic case is  $-0.6$  a.u. as it can be seen in the position of ATI peaks in the figures.
- (2) The molecular spectra are shown for forward-direction emission, while in the atomic

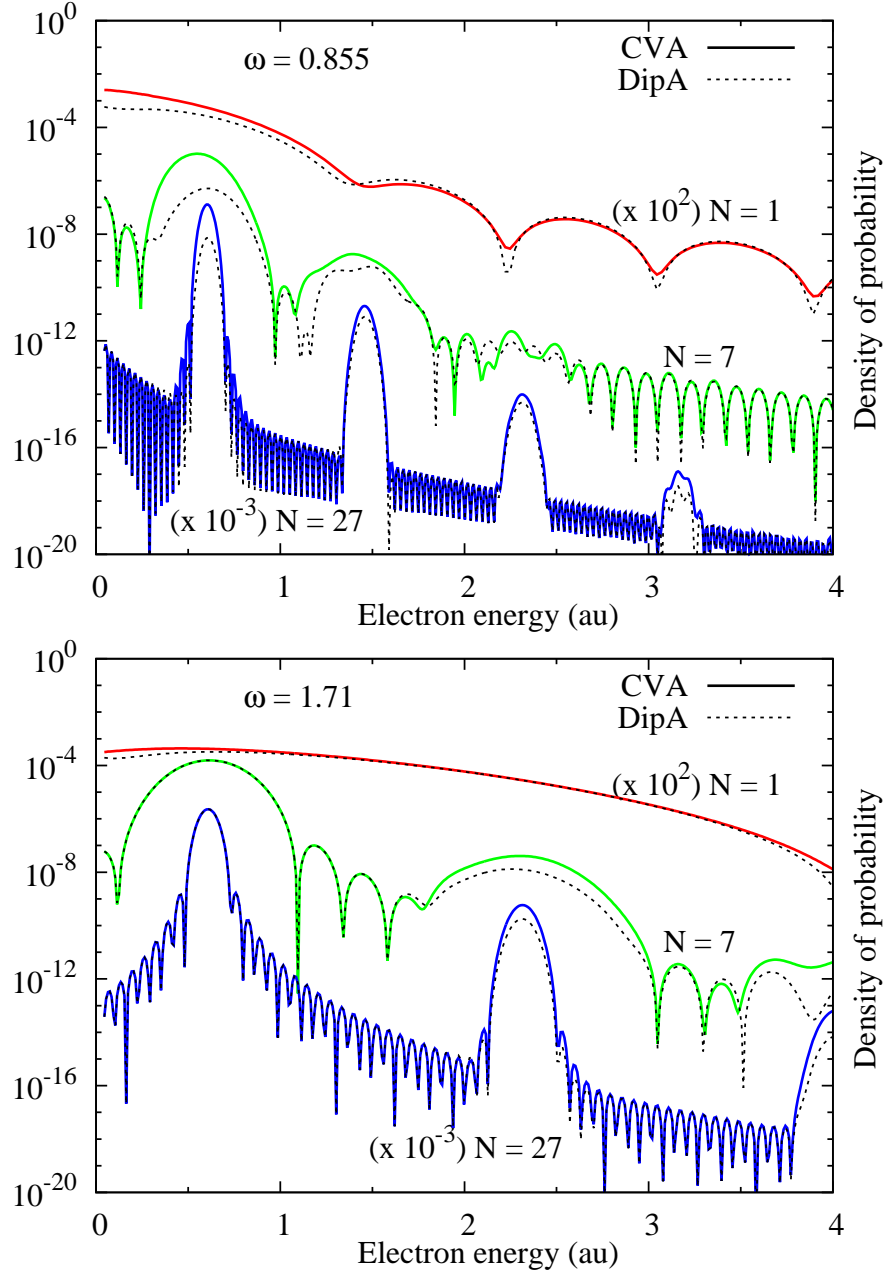


**Figure 8.** (colour online) Electronic spectra for ionisation of  $H_2^+(1s\sigma)$  as function of the electron energy, for emission in the forward direction. We have considered laser-pulses of  $N = 1, 7$ , and  $27$  cycles, with frequencies  $\omega = 0.855$  and  $1.71$  a.u., and an amplitude  $F_0 = 0.05$  a.u. Full line: CVA and dotted line: DipA.

case we have presented the probabilities integrated in emission direction. The principal difference is that the deep minima in the forward condition, similar to the atomic spectra for fixed direction  $\mathbf{k} \parallel \hat{\varepsilon}$  (not shown), are softened by integration on emission angles.

- (3) The agreement between CVA and DipA calculations is better in the atomic case. This fact can be understood since the  $1s\sigma$  orbital is more extended in space than the atomic  $1s$ . Then, for the same laser pulse, the approximation  $\mathbf{A} \cdot \mathbf{r} \ll 1$  is not satisfied in all range of the integral  $g(t)$ .

To analyse the emission in other directions we present in figure 9 the ionisation probabilities in three geometrical configurations: (a) in the forward direction, where the three vectors are parallel, i.e.  $\theta_R = \theta_k = 0$ , (b) with the electronic momentum parallel to the internuclear axis and both are at  $45^\circ$  respect to the polarisation vector, i.e.  $\theta_R = \theta_k = \pi/4$ , and (c) where the molecule is perpendicular to  $\hat{\varepsilon}$ ,  $\theta_R = 90^\circ$  and  $\theta_k = 45^\circ$ . In all theses cases the spectra are well reproduced by DipA (not shown). In particular, the arrangements (b) and (c) have the same contribution of  $\hat{\varepsilon} \cdot \mathbf{k}$ . Then, the factor  $\mathbf{M}^{(1)}$  is exactly the same in both cases, and all dependence of the spectra with the molecular orientation arises from the one-photon ionisation transition-matrix.

Similar conclusions can be deduced from the analysis of figure 10, where we compare the CVA results for ionisation from  $1s\sigma$ ,  $2p\sigma$ , in both cases with  $R = 2$  a.u. and from  $1s\sigma$  at  $R = 1.4$  a.u. This value is the equilibrium internuclear distance of the ground-state for the  $\text{H}_2$  molecule. As before, the differences are originated in the factor  $\mathbf{L}^{(1)}$ .

As concluded from the analysis on molecular ionisation, the dependence on the emission direction, molecular orientation, and molecular structure are derived from the one-photon transition matrix properties. These results are consistent with reports on several works of laser-pulse ionisation of  $\text{H}_2$  and  $\text{H}_2^+$  where the authors have observed coincidences with the one-photon case [63–65]. Our present work shows that the possibilities of finding “new molecular effects” due to the interaction with laser pulses should be investigated outside the range where DipA reproduces the exact spectra.

## 6. Conclusions

We have investigated ionisation of atomic and molecular ions of hydrogen, induced by short laser pulses from ground and some excited states. Differential and total ionisation probabilities were calculated using the Coulomb-Volkov (CVA) and DipA approximations proposed in this work. The accuracy of the proposed approximations was studied by comparing with numerically exact solutions of the TDSE. The present results show that the calculations accurately describe the ionisation probabilities in the range of laser parameters here explored.

DipA is deduced from the multipolar expansion of CVA T-matrix and therefore can be applied in the regime of validity of CVA, when is verified the condition  $\omega > I_p$ , while simultaneously being in the multiphotonic regime ( $\Gamma \gg 1$ ). The main feature of DipA is that it expresses the ionisation spectra as a product of two factors. One of them

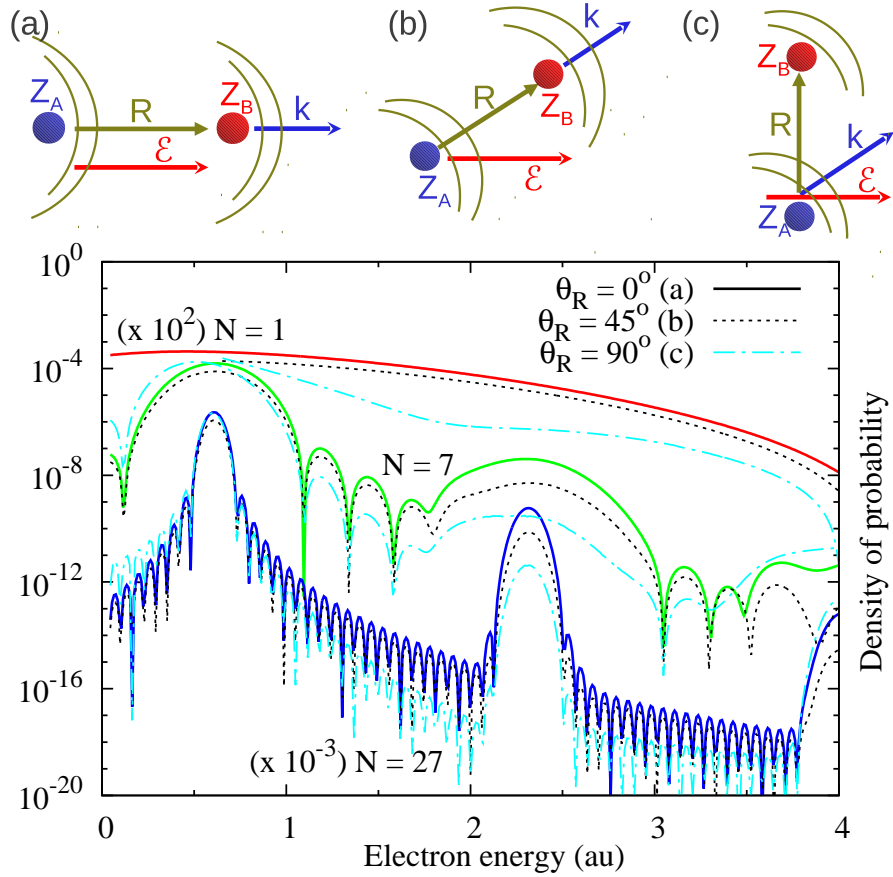


**Figure 9.** (colour online) CVA results for  $H_2^+$  ionisation spectra for the three geometrical arrangement: (a) forward configuration in solid line, (b)  $\mathbf{R} \parallel \mathbf{k}$  at  $45^\circ$  of  $\hat{\epsilon}$  in dotted line and (c)  $\mathbf{R} \perp \hat{\epsilon}$  and  $\mathbf{k}$  at  $45^\circ$  in dashed dotted line. The laser parameters are the same than in the bottom panel of figure 8.

accounts for the target structure and the ejected electron and is the well-known one-photon transition-matrix. The second factor depends comprises all the dependence on the laser-electron interaction and describes the main characteristics of the ATI spectra. Then, in this approximation laser and target contribute separately to the observed spectra.

We have proposed several applications of DipA, covering several aspects of the laser-matter interaction. such as the interpretation of the features of the ATI spectra that come from each contribution. Also, the proposed approximations to first and second order are concrete examples of computationally low-cost alternative methods to calculate differential and total cross-sections in complex atomic and molecular targets. In all cases we discussed the limits of validity and range of applicability of the approximations.

## 7. Acknowledgements

This work was partially supported by the Consejo Nacional de Investigaciones Científicas y Técnicas (Grant PIP 112-2009-0100166), Universidad Nacional de Cuyo (Grant

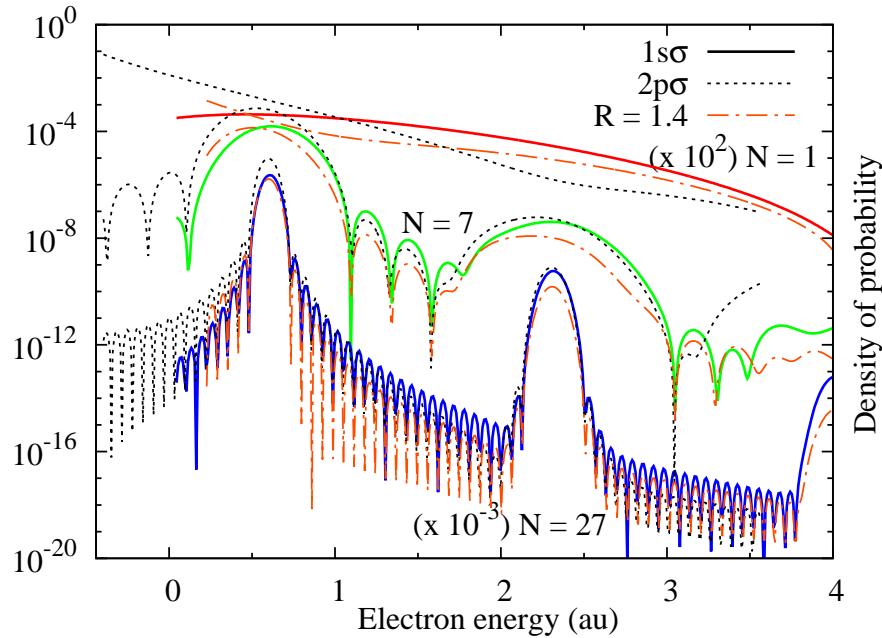


**Figure 10.** (colour online) CVA ionisation spectra for  $\text{H}_2^+$  in forward condition from (a)  $1s\sigma$  and  $R = 2$  a.u. in solid line, (b)  $2p\sigma$  and  $R = 2$  a.u. in dotted line, and (c)  $1s\sigma$  and  $R = 1.4$  a.u. in dashed-dotted line. The laser parameters are the same of figure 8. Curves (b) and (c) are shifted in energy.

06/C340), Argentina and from the EU Seventh Framework Programme under grant agreement PIRSES-GA-2010-269243.

## References

- [1] T. Brabec and F. Krausz. *Rev. of Mod. Phys.*, 72:545–591, 2000.
- [2] T. Brabec. *Strong field laser physics*. Springer, New York, 2008.
- [3] D. B. Milosevic, G. G. Paulus, D. Bauer, and W. Becker. *J. Phys. B: At. Mol. Opt. Phys.*, 39(14):R203–R262, 2006.
- [4] A. Becker and F. H. M. Faisal. *J. Phys. B: At. Mol. Opt. Phys.*, 38(3):R1–R56, 2005.
- [5] C. J. Joachain, M. Dörr, and N. Kylstra. High-intensity laser-atom physics. volume 42 of *Advances In Atomic, Molecular, and Optical Physics*, pages 225–286. Academic Press, 2000.
- [6] F. Krausz and M. Ivanov. *Review of Modern Physics*, 81:163–234, 2009.
- [7] P. B. Corkum and F. Krausz. *Nature Physics*, 3:381–387, 2007.
- [8] M. Hentschel, R. Kienberger, Ch. Spielmann, G. A. Reider, N. Milosevic, T. Brabec, P. Corkum, U. Heinzmann, M. Drescher, and F. Krausz. *Nature*, 414:509–513, 2001.
- [9] Kenneth C. Kulander. *Phys. Rev. A*, 36:2726–2738, 1987.
- [10] Kenneth C. Kulander. *Phys. Rev. A*, 35:445–447, 1987.

- [11] Dae-Il Choi and Will Chism. *Phys. Rev. A*, 66:25401, 2002.
- [12] D. Bauer and P. Koval. *Comput. Phys. Commun.*, 174:396–421, 2006.
- [13] A. N. Grum-Grzhimailo, B. Abeln, K. Bartschat, D. Weffen, and T. Urness. *Phys. Rev. A*, 81:43408, 2010.
- [14] Zhongyuan Zhou and Shih-I. Chu. *Phys. Rev. A*, 83:33406, 2011.
- [15] L. V. Keldysh. *Zh. Eksp. Teor. Fiz.*, 47:1945–1957, 1964.
- [16] F. H. M. Faisal. *J. Phys. B: At. Mol. Opt. Phys.*, 6(4):L89–L92, 1973.
- [17] Howard R. Reiss. *Phys. Rev. A*, 22:1786–1813, 1980.
- [18] L. I. Schiff. *Quantum Mechanics*. McGraw-Hill, New York, third edition, 1968.
- [19] G. Duchateau, C. Illescas, B. Pons, E. Cormier, and R. Gayet. *J. Phys. B: At. Mol. Opt. Phys.*, 33(16):L571–L576, 2000.
- [20] G. Duchateau, E. Cormier, H. Bachau, and R. Gayet. *Phys. Rev. A*, 63:53411, 2001.
- [21] R. Guichard, H. Bachau, E. Cormier, R. Gayet, and V. D. Rodríguez. *Physica Scripta Volume T*, 76:397–409, 2007.
- [22] G. Duchateau, E. Cormier, and R. Gayet. *Phys. Rev. A*, 66:23412, 2002.
- [23] D. G. Arbó, J. E. Miraglia, M. S. Gravielle, K. Schiessl, E. Persson, and J. Burgdörfer. *Phys. Rev. A*, 77:13401, 2008.
- [24] V. D. Rodríguez, D. G. Arbó, and P. A. Macri. *J. Phys. B: At. Mol. Opt. Phys.*, 44:5603, 2011.
- [25] G. Duchateau and R. Gayet. *Phys. Rev. A*, 65:13405, 2001.
- [26] V. D. Rodríguez, P. Macri, and R. Gayet. *J. Phys. B: At. Mol. Opt. Phys.*, 38(15):2775–2791, 2005.
- [27] V. D. Rodríguez. *Nuclear Instruments and Methods in Physics Research B*, 247:105–110, 2006.
- [28] R. Gayet. *J. Phys. B: At. Mol. Opt. Phys.*, 38(21):3905–3916, 2005.
- [29] V. D. Rodríguez, E. Cormier, and R. Gayet. *Phys. Rev. A*, 69:53402, 2004.
- [30] D. G. Arbó, M. S. Gravielle, K. I. Dimitriou, K. Tőkési, S. Borbély, and J. E. Miraglia. *The European Physical Journal D*, 59:193–200, 2010.
- [31] M. S. Gravielle, D. G. Arbó, J. E. Miraglia, and M. F. Ciappina. *J. Phys. B: At. Mol. Opt. Phys.*, 45:5601, 2012.
- [32] D. Dimitrovski, E. A. Solov’ev, and J. S. Briggs. *Phys. Rev. Lett.*, 93:83003, 2004.
- [33] D. Dimitrovski, E. A. Solov’Ev, and J. S. Briggs. *Phys. Rev. A*, 72:43411, 2005.
- [34] C. D. Lin, Anh-Thu Le, Zhangjin Chen, Toru Morishita, and Robert Lucchese. *J. Phys. B: At. Mol. Opt. Phys.*, 43:122001, 2010.
- [35] M. V. Frolov, N. L. Manakov, A. A. Silaev, N. V. Vvedenskii, and Anthony F. Starace. *Phys. Rev. A*, 83:21405, 2011.

- [36] M. V. Frolov, N. L. Manakov, T. S. Sarantseva, and Anthony F. Starace. *Phys. Rev. A*, 83:43416, 2011.
- [37] M. V. Frolov, D. V. Knyazeva, N. L. Manakov, A. M. Popov, O. V. Tikhonova, E. A. Volkova, Ming-Hui Xu, Liang-You Peng, Liang-Wen Pi, and Anthony F. Starace. *Phys. Rev. Letters*, 108:213002, 2012.
- [38] A.-T. Le, R. Della Picca, P. D. Fainstein, D. A. Telnov, M. Lein, and C. D. Lin. *J. Phys. B: At. Mol. Opt. Phys.*, 41(8):081002, 2008.
- [39] Guoli Wang, Cheng Jin, Anh-Thu Le, and C. D. Lin. *Phys. Rev. A*, 86:15401, 2012.
- [40] Zhangjin Chen, Anh-Thu Le, Toru Morishita, and C. D. Lin. *Phys. Rev. A*, 79:33409, 2009.
- [41] D. P. Dewangan and J. Eichler. *Comm. in At. and Mol. Phys.*, 27:317, 1992.
- [42] D. P. Dewangan and J. Eichler. *Phys. Rep.*, 247:59–219, 1994.
- [43] P. D. Fainstein, V. H. Ponce, and R. D. Rivarola. *J. Phys. B: At. Mol. Opt. Phys.*, 24(14):3091–3119, 1991.
- [44] R. Della Picca, P. D. Fainstein, and A. Dubois. *Phys. Rev. A*, 84:33405, 2011.
- [45] P. M. Paul, E. S. Toma, P. Breger, G. Mullot, F. Augé, Ph. Balcou, H. G. Muller, and P. Agostini. *Science*, 292(5522):1689–1692, 2001.
- [46] R. A. Bartels, A. Paul, H. Green, H. C. Kapteyn, M. M. Murnane, S. Backus, I. P. Christov, Y. Liu, D. Attwood, and C. Jacobsen. *Science*, 297(5580):376–378, 2002.
- [47] G. Sansone, E. Benedetti, F. Calegari, C. Vozzi, L. Avaldi, R. Flammini, L. Poletto, P. Villoresi, C. Altucci, R. Velotta, S. Stagira, S. De Silvestri, and M. Nisoli. *Science*, 314(5798):443–446, 2006.
- [48] Hiroki Mashiko, Steve Gilbertson, Chengquan Li, Sabih D. Khan, Mahendra M. Shakya, Eric Moon, and Zenghu Chang. *Phys. Rev. Letters*, 100:103906, 2008.
- [49] R. Kienberger, E. Goulielmakis, M. Uiberacker, A. Baltuska, V. Yakovlev, F. Bammer, A. Scrinzi, Th. Westerwalbesloh, U. Kleineberg, U. Heinzmann, M. Drescher, and F. Krausz. *Nature*, 427:817–821, 2004.
- [50] P. Billaud, M. Géléoc, Y. J. Picard, K. Veyrinas, J. F. Hergott, S. Marggi Poullain, P. Breger, T. Ruchon, M. Roulliay, F. Delmotte, F. Lepetit, A. Huetz, B. Carré, and D. Dowek. *J. Phys. B: At. Mol. Opt. Phys.*, 45:4013, 2012.
- [51] Willis E. Lamb. *Phys. Rev.*, 85:259–276, 1952.
- [52] R. Burlon, C. Leone, F. Trombetta Ferrante, and G. *Il Nuovo Cimento D*, 9:1033–1054, 1987.
- [53] D. Bauer, D. B. Milošević, and W. Becker. *Phys. Rev. A*, 72:23415, 2005.
- [54] H. R. Reiss. *Phys. Rev. A*, 76:33404, 2007.
- [55] Jingtao Zhang and Takashi Nakajima. *Phys. Rev. A*, 77:43417, 2008.
- [56] V. D. Rodríguez and R. O. Barrachina. *The European Physical Journal D*, 64:593–599, 2011.

- [57] G. Hadinger, M. Aubert-Frecon, and G. Hadinger. *J. Phys. B: At. Mol. Opt. Phys.* 22:697–712, 1989.
- [58] L. I. Ponomarev and L. N. Somov. *J. of Comput. Phys.*, 20:183, 1976.
- [59] J. Rankin and W. R. Thorson. *J. of Comput. Phys.*, 32:437, 1979.
- [60] P. M. Morse and H. Feshbach. *Methods of Theoretical Physics*. McGraw-Hill, New York, 1953.
- [61] R. Della Picca, P. D. Fainstein, M. L. Martiarena, and A. Dubois. *Phys. Rev. A*, 75(3):032710, 2007.
- [62] R. Della Picca, P. D. Fainstein, M. L. Martiarena, N. Sisourat, and A. Dubois. *Phys. Rev. A*, 79:32702, 2009.
- [63] Kai-Jun Yuan, Huizhong Lu, and André D. Bandrauk. *Phys. Rev. A*, 83:43418, 2011.
- [64] J. Fernández and L. B. Madsen. *J. Phys. B: At. Mol. Opt. Phys.* , 42:5602, 2009.
- [65] J. Fernández and L. B. Madsen. *Phys. Rev. A*, 79:63406, 2009.